e-ISSN: 2146 - 9067

International Journal of Automotive Engineering and Technologies

journal homepage:
https://dergipark.org.tr/en/pub/ijaet

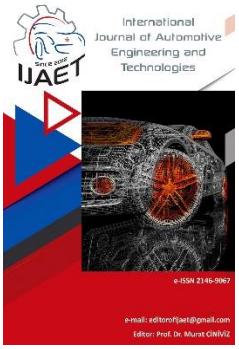

Original Research Article

Effects of Stroke to Bore Ratio on Exergy Balance in Spark Ignition Engines

İsmet Sezer[1, *]

[1, *] Mechanical Engineering Department, Gumushane University, 29100 Gumushane, Türkiye

ARTICLE INFO

Orcid Numbers
1. 0000-0001-7342-9172

Doi: 10.18245/ijaet.1084758

* Corresponding author
isezer@gumushane.edu.tr

Received: Mar 8, 2022
Accepted: May 15, 2023

Published: 30 Jun 2023

Published by Editorial Board Members of IJAET

ABSTRACT

This study aims to investigate theoretically the effects of stroke to bore ratio on exergy balance in spark ignition (SI) engines. For this purpose, a two–zone quasi–dimensional cycle model was developed for SI engines without considering the complex calculation of fluid dynamics. The combustion process is simulated as turbulent flame entrainment model in the cycle simulation. Principles of the second law of thermodynamics were applied to the developed model in order to perform the exergy (or availability) analysis. The variations of exergetic terms and irreversibilities throughout the investigated part of the cycle were analyzed depending on stroke to bore ratio. The results of the study showed that variation of stroke to bore ratio have significant effects on the variation of the exergetic terms, irreversibilities and efficiencies. Exergy transfer with work increases, while exergy transfer with heat decreases with increasing of stroke to bore ratio. The maximum increment in exergy transfer with work is about 12.5% and maximum decrement in exergy transfer with heat is about 11.25% for the stroke to bore ratio of 1.3 compared to stroke to bore ratio of 0.7. Irriversibilities and exergy transfer with exhaust decrease with the increasing of stroke to bore ratio. The maximum decrements are about 3.1% in the irriversibilities and 4.9% in exergy transfer with exhaust for the stroke to bore ratio of 1.3 compared to stroke to bore ratio of 0.7. The first and second law efficiencies are increase, while brake specific fuel consumption decreases with the increase of the stroke to bore ratio. The maximum increments are about 12.3% in the first and second law efficiencies and the maximum decrement is about 11.3% in brake specific fuel consumption for the stroke to bore ratio of 1.3 compared to stroke to bore ratio of 0.7.

Keywords: Spark ignition engine, Stroke to bore ratio, Exergy analysis, Irreversibilities, Efficiency

1. Introduction

The operating conditions and design parameters must be optimized to obtain the best desired outputs from internal combustion engines (ICEs) according to the properties of the used fuel. The experimental and simulation studies have shown that the variation of operating conditions engine speed, air–fuel ratio, combustion duration, valve overlap period and residual gas fraction etc. play an effective role on the heat release, cylinder pressure, peak pressure rise, and engine emissions [1]. In the recent times, the properly adjusting of the operating conditions is carried out by means of

electronic control units (ECUs) and the flexibility of the design parameters can be applicable via the use of the modified engine design i.e. variable stroke length, variable compression ratio, variable valve timing, supercharge and turbocharger [2]. Furthermore, the design parameters of the ICEs such as combustion chamber geometry, intake port diameter to bore ratio, cam profile, valve design, spark plug location, compression ratio, stroke to bore ratio (r_{sb}) etc. affect the combustion process, engine performance, vehicle fuel consumption and exhaust emissions characteristics. For that reason, numerous studies have been performed to investigate the effects of such design parameters on the various engine characteristics [3–7]. In most of these studies, thermodynamic based (zero– and quasi–dimensional) engine cycle models have been widely used to attain the required engine characteristics and assistance to new developments. The engine simulation models is a strong instrument for the researchers and designers because of its effectiveness to explore a new design before the production a prototype and perform the engine test [2]. However, the applied cycle simulations are generally based only on the first law of thermodynamics. But, in a few past decades, it has been clearly understood that the first law of thermodynamics alone is not capable of providing a suitable insight into the engine operations [8, 9]. For this reason, the interest in the use of the second law of thermodynamics has been intensified in the field of internal ICEs. Analysis of a process or a system by means of the second law of thermodynamics is termed exergy or exergy analysis. The application of exergy analysis for engineering systems proves to be very useful because it provides quantitative information about irreversibilities and exergy losses in the system. In this way, the thermodynamic efficiency can be quantified, poor efficiency areas can be identified, and thus processes can be designed and operated to be more efficient [10]. A series of papers was published on exergy analysis applied to ICEs, especially in a few last decades. From citing these papers, a review study was published by Caton in 2000 [11], and an extended one by Rakopoulos and Giakoumis in 2006 [9]. It has been seen from these review papers that numerous studies on the application of second law analysis to SI engines have been done especially recent years [12–17]. The effects of some design parameters have been investigated by means of exergy perspective in the a few exergy analysis studies devoted to ICEs. For example, the energy and exergy analyses were performed by Sohret et al. [18] based on experimental results conducted on hydrogen fuelled a single cylinder, air cooled spark ignition (SI) engine which was operated with the lean mixture at 1600 rpm constant engine speed and wide–open throttle conditions under various compression ratios and spark ignition timing. They declared that the experimental results obtained from energy and exergy analyses showed that the increase in compression ratio gave an increase in indicated and effective performance parameters of the engine while decrease in exergy destruction. In another study performed by Sezer and Bilgin [19], the effects of compression ratio was also examined by means of exergy analysis. They stated that increasing of compression ratio resulted in increase in the first and second law efficiencies and decrease in irreversibilities. However, effects of stroke to bore ratio have not been studied from the standpoint of exergy analysis. For this reason, this study aims to make a contribution by filling this gap in the literature via the investigation of the stroke to bore ratio effects on the exergy balance in SI engines.

2. Mathematical Model

2.1. Governing equations of cycle model

A quasi–dimensional thermodynamic cycle model which is mainly based on the firstly presented model by Ferguson [20] has been used in this study. Equations of the original model have been rearranged for the used model. The governing equations of the cycle model were derived from the first law of thermodynamics (the energy equation) by assuming that the cylinder content complies the ideal gas law. The energy equation in crank angle basis is arranged as follow.

$$\Delta E_{\text{int}} = Q - W \Rightarrow$$

$$m\frac{de_{\text{int}}}{d\theta} + e_{\text{int}}\frac{dm}{d\theta} = \frac{dQ}{d\theta} - p\frac{dV}{d\theta} \quad (1)$$

Here; m is the mass of cylinder content, e_{int} is the specific internal energy, Q is the heat transfer, p is pressure, V is volume, and θ is the

crank angle. Eq. (1) shows the variations of the thermodynamic properties respect to the crank angle. Moreover, these thermodynamic properties are also functions of temperature and pressure, which are determined in the model.

To determine instantaneous cylinder volume, pressure, burned and unburned gas temperatures, the following governing equations have been used in the presented model.

$$V(\theta)=V_{cc}\left\{1+\frac{r_{comp}-1}{2}\left[1-cos\theta+\frac{1}{r_{cr}}\left[1-\left(1-r_{cr}^{2}sin^{2}\theta\right)^{0.5}\right]\right]\right\} \quad (2)$$

Here; r_{comp} is the compression ratio, r_{cr} is half of the ratio of stroke length (L_s) to connecting rod length (L_{cr}) and it is defined as $r_{cr}= L_s /2L_{cr}$.

$$\frac{dp}{d\theta}=\frac{A+B+C}{D+E} \quad (3)$$

$$A=\frac{1}{m}\frac{dV}{d\theta}$$

$$B=\frac{\lambda_g}{\omega m}\left[\frac{v_b}{C_{p,b}}\frac{\partial \ln v_b}{\partial \ln T_b}\left(1-\frac{T_{cw}}{T_b}\right)A_b+\frac{v_u}{C_{p,u}}\frac{\partial \ln v_u}{\partial \ln T_u}\left(1-\frac{T_{cw}}{T_u}\right)A_u\right]$$

$$C=-\frac{dr_{mbf}}{d\theta}\left[(v_b-v_u)+v_b\frac{\partial \ln v_b}{\partial \ln T_b}\frac{h_b-h_u}{C_{p,b}T_b}\right]$$

$$D=r_{mbf}\left[\frac{v_b^2}{C_{p,b}T_b}\left(\frac{\partial \ln v_b}{\partial \ln T_b}\right)^2+\frac{v_b}{p}\frac{\partial \ln v_b}{\partial \ln p}\right]$$

$$E=\left(1-r_{mbf}\right)\left[\frac{v_u^2}{C_{p,u}T_u}\left(\frac{\partial \ln v_u}{\partial \ln T_u}\right)^2+\frac{v_u}{p}\frac{\partial \ln v_u}{\partial \ln p}\right]$$

$$\frac{dT_b}{d\theta}=\frac{-\lambda_g A_b\left(T_b-T_{cw}\right)}{\omega m C_{p,b}r_{mbf}}+\frac{v_b}{C_{p,b}}\frac{\partial \ln v_b}{\partial \ln T_b}\frac{dp}{d\theta}+\frac{h_u-h_b}{r_{mbf}C_{p,b}}\frac{dr_{mbf}}{d\theta} \quad (4)$$

$$\frac{dT_u}{d\theta}=\frac{-\lambda_g A_u\left(T_u-T_{cw}\right)}{\omega m C_{p,u}\left(1-r_{mbf}\right)}\frac{dp}{d\theta}+\frac{v_u}{C_{p,u}}\frac{\partial \ln v_u}{\partial \ln T_u} \quad (5)$$

It is also used the extra governing equations to compute the work output and heat loss.

$$\frac{dW}{d\theta}=p\frac{dV}{d\theta} \quad (6)$$

$$\frac{dQ_{cw}}{d\theta}=\frac{\lambda_g}{\omega}\left[A_b\left(T_b-T_{cw}\right)+A_u\left(T_u-T_{cw}\right)\right] \quad (7)$$

In above equations, A_b and A_u are also the wetted areas by burned and unburned gases, which are computed from the geometrical sub–model given as follow. Angular speed (ω), cylinder wall temperature (T_{cw}) and heat transfer coefficient (λ_g) are determined as follow.

$$\omega=\frac{2\pi n}{60} \quad (8)$$

$$T_{cw}=T_{cf}+R_{cw}\frac{dQ_{cw}}{d\theta} \quad (9)$$

$$\lambda_g=3.26\,D_c^{-0.2}p^{0.8}T^{-0.55}U_g^{0.8} \quad (10)$$

In the equations above; U_g is the velocity of the gases in the cylinder, T_{cf} is the cooling fluid temperature and R_{cw} is the thermal resistance coefficient of the cylinder walls. The values of T_{cf} = 350 K and R_{cw} = 0.01 K/W are used in the cycle model.

Further details of the cycle model can be found in references [20, 21].

2.2. Combustion model

After the initiation of combustion at a specified crank angle, it is assumed that two–zones namely burned and unburned zones exist in the combustion chamber. The each zone is assumed to be uniform in temperature and homogenous in composition. It is also assumed that uniform pressure distribution exists in whole cylinder. The combustion process is simulated as the turbulent flame propagation and it is supposed that flame front progressive spherically in the unburned gases. Under these assumptions, the following governing equations, which were firstly presented by Blizard and Keck [22, 23], then developed by Tabaczynski *et al.* [24] and Tabaczynski *et al.* [25] and recently used by Bayraktar and Durgun [26] were used to determine the burnt mass fraction in the combustion model.

$$\frac{dm_e}{d\theta}=\rho_u A_f U_e \quad (11)$$

$$\frac{dm_b}{d\theta}=\rho_u A_f U_L+\frac{m_e-m_b}{\tau_{bd}} \quad (12)$$

$$\tau_{bd}=\frac{l_T}{U_L} \quad (13)$$

Here; A_f is area of the flame front and τ_{bd} is the characteristic burn duration of an eddy at size of l_T.

The rate of mass burned is proportional to the flame front area and flame speed. The flame

front area A_f is computed instantaneously depending on enflamed volume V_f by means of the geometrical sub–model given below. The following equations are also used to compute the turbulent entrainment speed U_e, turbulent speed U_T and the characteristic length scale of turbulent flame l_T.

$$U_e = U_T + U_L \tag{14}$$

$$U_T = 0.08\bar{U}_{ind}\left(\frac{\rho_i}{\rho_e}\right)^{1/2} \tag{15}$$

$$\bar{U}_{ind} = \eta_v\left(\frac{A_{pc}}{A_{iv,max}}\right)\frac{nL_s}{30} \tag{16}$$

$$l_T = 0.8L_{iv,max}\left(\frac{\rho_e}{\rho_{ind}}\right)^{3/4} \tag{17}$$

Here; $\bar{U}_{ind}$ is the mean speed of entering gases to cylinder during induction period, A_{pc} is the area of piston crown, $A_{iv,max}$ is the maximum opening area of intake valve and $L_{iv,max}$ is maximum intake valve lift.

Laminar flame speed (U_L) is the velocity at which the flame propagates into quiescent premixed unburned mixture ahead of the flame. U_L is calculated as the equations presented by Gülder [27].

$$U_L(\phi, T, p) = U_{L,0}\left(\frac{T_u}{T_0}\right)^{\delta}\left(\frac{p}{p_0}\right)^{\varphi}(1-\psi f) \tag{18}$$

Here; $U_{L,0}$ is the laminar flame speed at standard conditions of T_0=298 K and p_0=1 bar for a given mixture strength. ϕ_0, δ and φ are constants or mixture strength dependent terms.

$U_{L,0}$ is also calculated as follow.

$$U_{L,0}(\phi) = \Phi\Omega\phi^{\sigma}\exp\left[-\xi\left(\phi-1.075\right)^2\right] \tag{19}$$

The values of δ, φ, Φ, Ω, σ and ξ can be found in literature [27] and ψ is taken as 2.5 for $0 \le f \ge 0.3$. f is the mass fraction of the residual gas.

2.3. Geometric sub–model

In the geometric sub–model, it is supposed that the spherical flame propagation from the spark plug throughout the combustion chamber as seen in Fig. 1.

Depends on this assumption, the enflamed volume V_f, the flame surface area A_f and the total heat transfer surface area $A_{w,tot}$ are computed as the instantaneous enflamed volume V_f and combustion chamber height h_{cc} by using of an iterative method. The values of V_f and h_{cc} have been determined from thermodynamic cycle model as follow.

$$V_f(\theta) = V_b(\theta) + \frac{\left[m_e(\theta) - m_b(\theta)\right]}{\rho_u} \tag{20}$$

$$h_{cc}(\theta) = L_s\left[\frac{1}{\left(r_{comp}-1\right)}\right] + 0.5\left[1-\cos(\theta)\right] \tag{21}$$

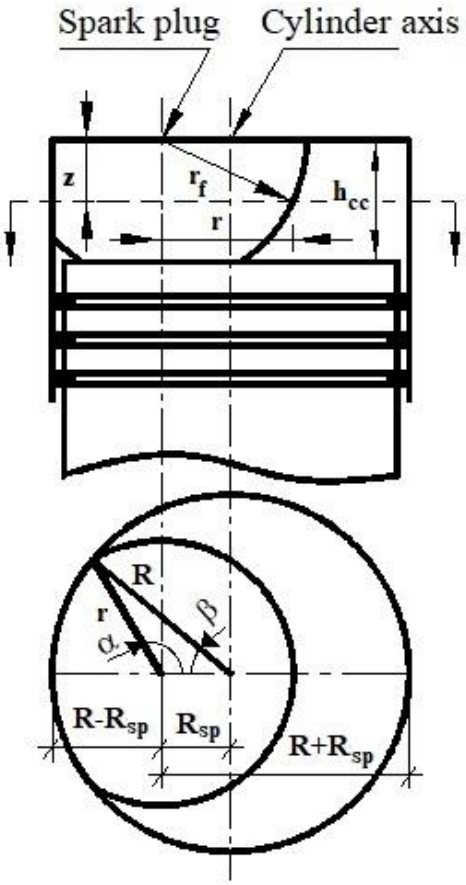

Fig. 1. Flame front geometry [28]

The geometric features of flame front seen in Fig. 1 have been determined for any flame radius from the following mathematical relations [22, 23, 28].

$$A_f(r_f) = 2r_f\int_{z=0}^{z=y}\alpha(z)\,dz \tag{22}$$

$$V_f(r_f) = 2r_f\int_{z=0}^{z=y}\left[\alpha(z)\,r^2(z) + \beta(z)R^2 - r_{sp}R\sin\beta(z)\right]dz \tag{23}$$

Here;

$$cos\alpha = \left(r_{sp}^2 + r^2(z) - R^2\right)/\left[2r_{sp}r(z)\right];$$

$$cos\beta = \left(r_{sp}^2 + r^2(z) - R^2\right)/\left[2r_{sp}r(z)\right];$$

$$r^2(z) = r_f^2 - z^2.$$

The total combustion chamber area wetted by burned gases is the sum of the areas of the cylinder head, cylinder wall and piston crown wetted by the burned gases and it is determined as follow.

$$A_{w,tot}(r_f) = A_{w,ch}(r_f) + A_{w,cw}(r_f) + A_{w,pc}(r_f) \quad (24)$$

$$A_{w,ch}(r_f) = \alpha(0)r^2(0) + \beta(0)R^2 - r_{sp}R\sin\beta(0) \quad (25)$$

$$A_{w,cw}(r_f) = 2\int_{z=0}^{z=y} R\beta(z)\,dz \quad (26)$$

$$A_{w,pc}(r_f) = \alpha(y)r^2(y) + \beta(y)R^2 - r_{sp}R\sin\beta(y) \quad (27)$$

The wetted area by the unburned gases is determined via the assumption of total combustion chamber area is the sum of areas contact with the burned and unburned zones as follow.

$$A_{w,tot} = A_b + A_u \quad (28)$$

2.4. Computation of the cycle

As well known, spark ignition engine cycles consist of four consecutive processes namely induction, compression, expansion and exhaust. The thermodynamic properties during intake and exhaust processes are computed via the approximation method presented by Bayraktar and Durgun [26]. In this method, the pressure loss during intake process is computed by means of Bernoulli equation for one dimensional uncompressible flow thus pressure and temperature of intake charge (fuel–air mixture) are determined as follow.

$$P_{ind} = p_0 - \Delta p_{ind} \quad (29)$$

$$T_{ind} = \frac{(T_0 + \Delta T_{ind} + r_{rg}T_{exh})}{(1 + r_{rg}T_{exh})} \quad (30)$$

Here; p_0 and T_0 are the ambient pressure and temperature. Δp_{ind} is the pressure loss during intake period and ΔT_{ind} is the variation in temperature of intake charge.

Engine volumetric efficiency is computed as follow.

$$\eta_v = \gamma_{sc}\left(\frac{r_{comp}}{r_{comp}-1}\right)\left(\frac{p_{ind}}{p_0}\right)\left(\frac{T_0}{T_0 + \Delta T + r_{rg}T_{exh}}\right) \quad (31)$$

Here; γ_{sc} is the coefficient of supercharge and r_{rg} is the molar ratio of the residual gases.

The compression, combustion and expansion periods are computed by the organization of governing equations between (3)–(7) for an each process in a suitable way.

Exhaust pressure p_{exh} and exhaust temperature T_{exh} are also computed from the following equations as follow depending on the ambient pressure p_0 and temperature of burned gas T_b.

$$p_{exh} = (1.05 \approx 1.25)\,p_0 \quad (32)$$

$$T_{exh} = \frac{T_b}{(p_b / p_{exh})^{1/3}} \quad (33)$$

One time the computation of cycle was completed, the engine performance parameters, i.e., brake mean effective pressure (BMEP), brake thermal efficiency (BTE) and brake specific fuel consumption (BSFC) have been determined from the well–known equations in Refs. [20, 21, 26].

2.5. The second law (exergy) concept

The second law is an analogous the statement of entropy balance as follow [10, 29].

$$\Delta S = \int\left(\frac{Q}{T}\right)_{boundary} + S_{int} \quad (34)$$

Here; S_{int} is the total entropy generation due to the internal irreversibilities.

Considering the combination of the first and second law of thermodynamics availability namely exergy equation can be stated for a closed system as follow [10, 29].

$$E = E_{tot} + p_0 V - T_0 S \quad (35)$$

Here; E_{tot} is the total energy which is sum of internal, kinetic and potential energies ($E_{tot}=E_{int}+E_{kin}+E_{pot}$), V and S are volume and entropy of the system, respectively, and p_0 and T_0 are the fixed pressure and temperature of the dead state.

Availability (or exergy) is described as the maximum theoretical work that can be obtained from a combined system (combination of a system and its reference environment) when the system comes into equilibrium (as thermally, mechanically and chemically) with the environment [9, 10, 11, 29, 30]. The maximum available work from a system emerges as the sum of two contributions; thermomechanical exergy X_{tm} and chemical exergy X_{chem}. Thermomechanical exergy is described as the maximum extractable work from the combined

system when the system comes into thermal and mechanical equilibrium with the environment and it is determined as follow [9, 10, 31].

$$X_{tm} = E_{tot} + p_0 S - \Sigma \mu_{0,i} m_i \quad (36)$$

Here; m_i and $\mu_{0,i}$ are the mass and chemical potential of each species (i) calculated at the restricted dead state conditions.

At the restricted dead state conditions, the system is in thermal and mechanical equilibrium with the environment and no work potential exists between the system and environment due to temperature and pressure differences. But, the system does not reach the chemical equilibrium with the environment because the contents of the system are not permitted to mix with the environment or enter the chemical reaction by environmental components [31]. In principle, the difference between the compositions of the system at the restricted dead state conditions and the environment can be used to obtain extra work to reach the chemical equilibrium. The maximum work obtained in this way is called as chemical exergy and it is determined as follow [9, 10, 31].

$$X_{chem} = \sum m_i \left(\mu_{0,i} - \mu_i^0 \right) \quad (37)$$

Here; μ_i^0 is the chemical potential of each species (i) calculated at exact dead state conditions.

Exergy balance for a closed system for any process can be also written as follow [11, 32, 33].

$$\Delta X_{tot} = X_{2,tot} - X_{1,tot} = X_Q - X_W - X_{dest} \quad (38)$$

Here; ΔX_{tot} is the variation of the total system exergy, $X_{2,tot}$ is the total exergy at the end of the process, $X_{1,tot}$ is the total exergy at the start of the process, X_Q is the exergy transfer via heat transfer interactions, X_W is the exergy transfer via work interactions, and X_{dest} is the destroyed exergy by the irreversible processes.

Taking into account of fuel chemical exergy, exergy balance equation for an engine cylinder is written as follow [21, 34].

$$\frac{dX_{tot}}{d\theta} = \left(1 - \frac{T_0}{T}\right)\frac{dQ}{d\theta} - \left(\frac{dW}{d\theta} - p_0 \frac{dV}{d\theta}\right) + \frac{m_f}{m_{tot}} \frac{dr_{mbf}}{d\theta} x_{f,chem} - \frac{dI_{comb}}{d\theta} \quad (39)$$

The left–hand side of Eq. (39) is the rate of change in total exergy of cylinder contents. The first and second terms on the right–hand side represents the exergy transfer with heat and the exergy transfer with work. The third term on the right–hand side corresponds to the burned fuel exergy. Here; m_f and m_{tot} are the masses of the fuel and total cylinder contents and $x_{f,chem}$ is the specific fuel chemical exergy.

The total fuel chemical exergy ($X_{f,chem}$) is calculated from the following equation that is developed for liquid fuels by Kotas [35].

$$X_{f,chem} = x_{f,chem} m_f = Q_{LHV}\left[1.0401 + 0.01728\frac{h'}{c'} + 0.0432\frac{o'}{c'} + 0.2196\frac{s'}{c'}\left(1 - 2.0628\frac{h'}{c'}\right)\right] \quad (40)$$

Here; Q_{LHV} is lower heating value of fuel and it is calculated from the Mendeleyev formula as follow.

$$Q_{LHV} = \left[33.91c' + 125.6h' - 10.89(o' - s') - 2.51(9h' - w')\right] \quad (41)$$

In Eqs. (40) and (41); the variables of h', c', o', s' and w' represent mass fractions of elements carbon, hydrogen, oxygen, sulfur and the water in the fuel, respectively.

The last term on the right–hand side of Eq. (39) illustrates the exergy destruction in a cylinder due to combustion and it is calculated as follow.

$$\frac{dI_{comb}}{d\theta} = T_0 \frac{dS_{comb}}{d\theta} \quad (42)$$

Here; $dS_{comb}/d\theta$ is the rate of entropy generation due to combustion irreversibilities and it is computed from two–zone combustion model depending on entropy balance as follow [17, 30].

$$\frac{dS_{comb}}{d\theta} = \frac{d(m_b s_b)}{d\theta} + \frac{d(m_u s_u)}{d\theta} \quad (43)$$

Here; m_b and m_u are the burned and unburned masses of the cylinder contents and s_b and s_u are the specific entropy values of the burned and unburned gases.

Entropy production sourced from heat transfer process is determined as in Eq. (44) and exergy destruction due to heat transfer has been already determined as in Eq. (39).

$$\frac{dS_Q}{d\theta} = \left(\frac{dQ_b/d\theta}{T_b}\right) + \left(\frac{dQ_u/d\theta}{T_u}\right) \quad (44)$$

Here; $(dQ_b/d\theta)$ and $(dQ_u/d\theta)$ are the rates of heat loss from the burned and unburned gas zones at temperatures of T_b and T_u, respectively. Moreover, the total exergy destruction considered here is consists of combustion and also heat transfer irreversibilities and it is

computed as follow [17].

$$\frac{dI_{\text{tot}}}{d\theta} = \frac{dI_{\text{comb}}}{d\theta} + \frac{dI_{\text{Q}}}{d\theta} \tag{45}$$

The efficiency is defined to be able to compare different engine size applications or evaluate various improvement effects from the perspective of either the first or the second law of thermodynamics [9]. The first law (or energy based) efficiency is defined as follow.

$$\eta_{\text{I}} = \frac{Energy\ out\ \left(as\ work\right)}{Energy\ in} = \frac{W}{m_{\text{f}}\ Q_{\text{LHV}}} \tag{46}$$

Here; W is the engine indicated work output.
The various second law efficiencies (exergetic or exergy efficiency, or effectiveness) have been defined in the literature [20, 21]. In this study, the following description is preferred to determine the second law efficiency.

$$\eta_{\text{II}} = \frac{Exergy\ out\ \left(as\ work\right)}{Exergy\ in} = \frac{X_{\text{W}}}{m_{\text{f}}\ x_{\text{f,chem}}} \tag{47}$$

Here; X_{W} is the exergy transfer with work.

3. Numerical Applications

3.1. Computer program and solution procedure

A computer code has been written for the presented SI engine cycle model. Input parameters in the software were r_{comp}, n, ϕ, r_{sp}, θ_{st}, properties of fuel, ambient pressure and temperature. Once determining the intake conditions, the thermodynamic state of the cylinder charge is predicted by solving the governing differential equations. To integrate these differential equations, DVERK subroutine is used. The composition and thermodynamic properties of cylinder content in the simulation are computed by FORTRAN subroutines FARG (fuel–air–residual gas) and ECP (equilibrium–combustion–products), which were originally developed by Ferguson [20]. Exergetic calculations are performed as simultaneously depending on thermodynamic state of the cylinder content.
Finally, the results obtained have been corrected as the error analysis as follow [20, 21].
By fixing the values of ε_1 and ε_2 at 10^{-4} level, the confidence of the analysis and the cycle simulation program is fulfilled.

$$\varepsilon_1 = 1 - \left(\frac{vm}{V}\right) \tag{48}$$

$$\varepsilon_2 = 1 + \left[\frac{W}{\Delta(mu)} + Q_{\text{cw}}\right] \tag{49}$$

3.2. Validation of the model

To demonstrate the reliability of the presented cycle model, the predicted values are compared with experimental data in Fig. 2 (a) and (b) for the conditions specified on the figure and engine specifications given in Table 1. As can be seen in the figures, predictions for cylinder pressure and mass fraction burned curves are in good agreement with the experimental data. Therefore, the presented model has an enough level of confidence for analysis of engine performance and parametric investigation studies.

Table 1. The specifications of the experimental engines

Specification	Engine I [12]	Engine II [22]
r_{comp}	7	5
r_{sp}	0.1	0.3
D_{c} [mm]	76.2	63.5
L_{s} [mm]	111.125	76.2
L_{cr} [mm]	220	127
d_{iv} [mm]	30	25
$L_{\text{iv,max}}$ [mm]	4.2	4.8

4. Results and Discussion

Fig. 3 shows typical variations of the exergetic terms during the investigated part of the cycle for the conditions given in the figure. As seen in Fig. 3, thermomechanical exergy (X_{tm}) increases gradually during compression stroke up to the beginning of combustion while fuel chemical exergy ($X_{\text{f,chem}}$) remains constant. During compression period, the increasing of the thermomechanical exergy is directly related to the exergy transfer with work (X_{W}) which has a symmetrical variation by thermomechanical exergy with a negative sign. However, there is no evident variation in irreversibilities (I) due to a negligible exergy transfer with heat (X_{Q}) in this period. The variation in the total exergy (X_{tot}) reflects the variation in the thermomechanical exergy. With the start of combustion, at the crank angle of –30 degrees before top dead center (°BTDC), fuel chemical exergy decreases rapidly because of the conversion to heat. In consequence of this conversion, i.e., combustion of fuel, temperature

and pressure increase in the cylinder, which results in a steep increase in thermomechanical exergy and increase in exergy transfer with heat from cylinder contents to the walls.

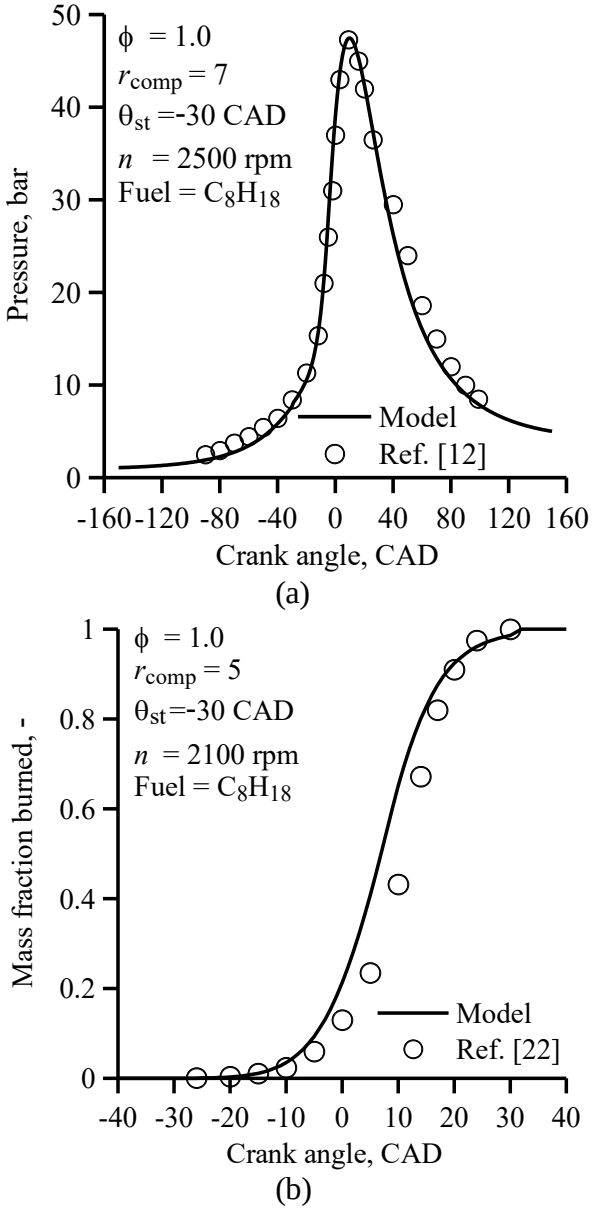

Fig. 2. Comparison of the predicted values with experimental data

Both of the heat transfer and especially combustion give a rapid increase in irreversibilities due to entropy generation during combustion. Combustion period ends at the crank angle of 34 degrees after top dead center (°ATDC) and expansion process continues until the piston reaches the bottom dead center (BDC). During this part of the cycle namely expansion period, decreases in X_{tm} and X_{tot} continues due to the exergy transfers from the system (cylinder) both of work and heat, while irreversibilities stand almost at a constant level. The remaining exergy in the cylinder at the end of expansion period emits with exhaust gases, which called as exergy transfer with exhaust (X_{exh}). The distributions of exergetic terms in fuel chemical exergy, i.e., X_Q, X_W, X_{exh} and I were computed about 8%, 36.5%, 36.9% and 18%, respectively for the conditions in Fig. 3.

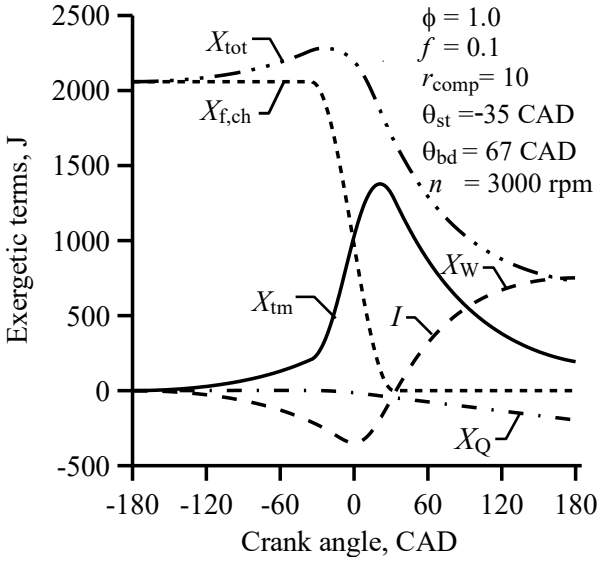

Fig. 3. Typical variation of the exergetic terms

Three different cylinders having the same displacement volume (400 cm^3) and different r_{sb} values have been studied in exergy analysis. Values of r_{sb} given in Table 2 are used as given in Ref. [5].

Table 2. Engine specifications used for exergy analysis [5]

Description	Values		
Stroke to bore ratio (r_{sb})	0.7	1.0	1.3
Stroke length (L_s), mm	62.8	79.5	95.5
Cylinder diameter (bore) (D_c), mm	90	80	73
Connecting rod length (L_{cr}), mm	126	159	191
Compression ratio (r_{comp})	9	9	9
Intake valve head diameter (d_{iv}), mm	39.4	35	32
Maximum valve lift ($L_{iv,max}$), mm	1.007	8.95	8.17
Displacement volume (V_d), cm^3	400	400	400
Combustion duration (θ_{bd}), CAD	134	92	74

Fig. 4 shows the effects of r_{sb} on exergy transfer with heat. As seen in the figure, exergy transfer with heat increases with the decreasing of r_{sb} and thus it reaches the maximum values for the r_{sb} of 0.7. It is considered that the increment in X_Q is sourced from the increase of combustion

duration when the r_{sb} decreases. As seen in Table 2, combustion durations are about 134, 92 and 74 CAD for the r_{sb} values of 0.7, 1.0, and 1.3, respectively. The increasing of combustion duration creates naturally more exergy transfer with heat because the heat transfer duration extends. Additionally, it is believed that increment of cylinder surface area with the decreasing the r_{sb} is another reason for the increments in exergy transfer with heat. The decreases in exergy transfer with heat are computed about 3 and 11.25 % for r_{sb} values of 1.0 and 1.3 in compared with that of the r_{sb} value of 0.7.

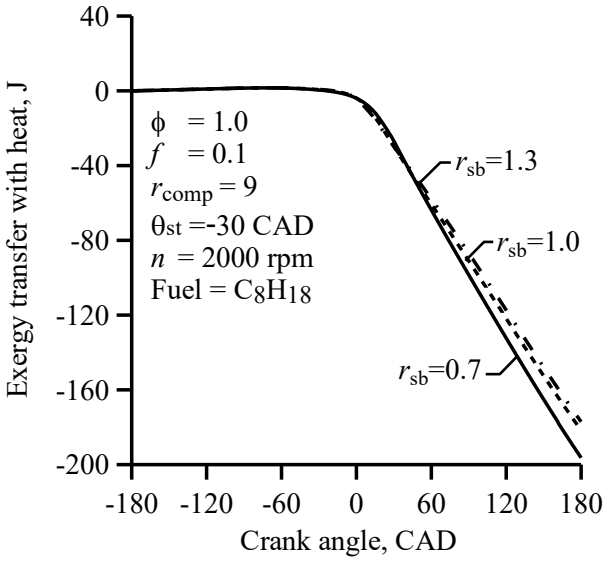

Fig. 4. Effects of r_{sb} on the exergy transfer with heat

Fig. 5 shows the effects of r_{sb} on the exergy transfer with work. As seen in the figure, exergy transfer with work increases with increasing of r_{sb} and thus it reaches the maximum values for the r_{sb} value of 1.3. It is considered that increment in X_W is obtained with the increase of r_{sb} because of the increase of the engine stroke length. The increment of engine stroke length provides the more exergy transfer with work by extending the expansion period as expected. On the other hand, it is believed that decrease of exergy transfer with heat with the increase of r_{sb} supplies to obtain the more exergy transfer with work. Increases in exergy transfer with work are computed about 9.3 and 12.5 % for the r_{sb} values of 1.0 and 1.3 in comparison with that of the r_{sb} value of 0.7.

Fig. 6 shows the effects of r_{sb} on the irriversibilities. As seen in the figure, the irriversibilities increases with decreasing of r_{sb} and thus it reaches the minimum values for the r_{sb} of 1.3. As mentioned before, the irriversibilities are the sum of combustion and heat transfer irriversibilities. As expected, combustion irreversibility increases with the extended combustion duration and heat transfer irreversibility increases with the increase of heat transfer as a result of the more entropy generation. Therefore, the irriversibilities sourced from combustion and heat transfer decrease with the decreasing of r_{sb} because of the decreasing of combustion duration as seen in Table 2. The decreases in irriversibilities are computed about 2.5 and 3.1 % for r_{sb} values of 1.0 and 1.3 in compared to that of the r_{sb} value of 0.7.

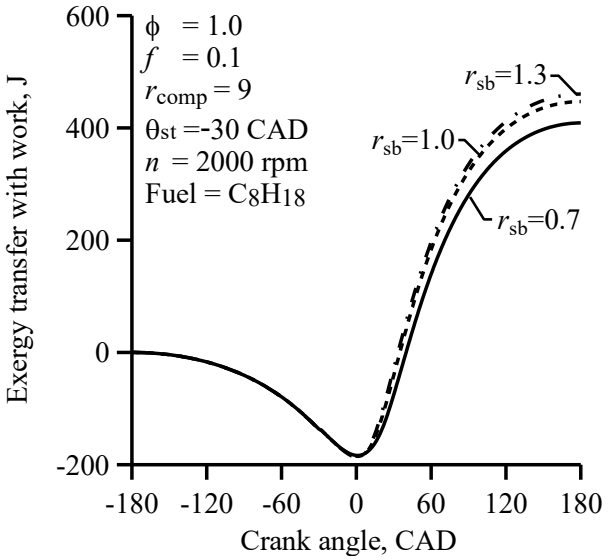

Fig. 5. Effects of r_{sb} on the exergy transfer with work

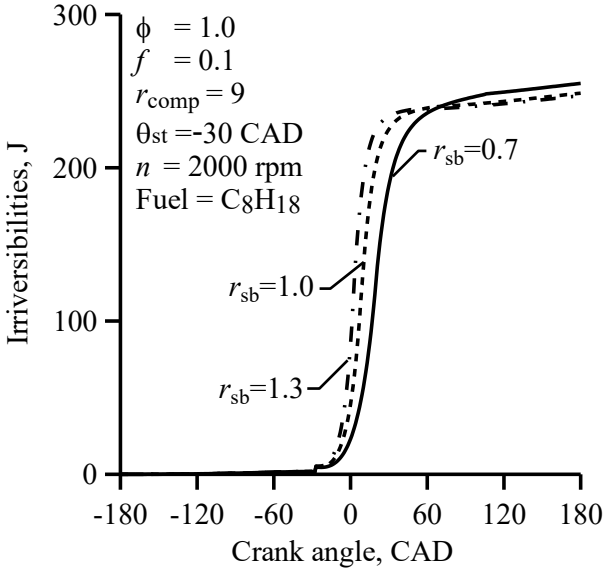

Fig. 6. Effects of r_{sb} on the irriversibilities

Fig. 7 indicates the effects of r_{sb} on the thermomechanical exergy. As seen in the figure, thermomechanical exergy increases during

compression and combustion periods due to increase of pressure and temperature in the cylinder, while it decreases during expansion process because of the reduction of cylinder pressure and temperature. With the changing of r_{sb}, the different variations appear in thermomechanical exergy during combustion and expansion periods due to different combustion durations. As expected, the variation of combustion duration affects the pressure and temperature histories in the cylinder. The shortening of combustion duration with the decrease of r_{sb} generates the higher cylinder pressure and temperature during combustion period, thus thermomechanical exergy increases in this period. On the other hand, thermomechanical exergy decreases more quickly with the decrease of r_{sb} because the cylinder pressure and temperature drop earlier during expansion process by reason of the short–term combustion.

Fig. 8 indicates the effects of r_{sb} on the fuel chemical exergy. As seen in the figure, the fuel chemical exergy remains stable during compression period and it begins to decrease rapidly with the start of combustion due to chemical energy of the fuel is converted to heat by means of combustion. Then, fuel chemical exergy reaches the zero at the end of the combustion period for the stoichiometric or lean fuel–air mixtures. On the other hand, some fuel chemical exergy remains as waste exergy at the end of combustion when using the rich fuel–air mixtures, since all of the fuel is not burned during combustion. The variation in the fuel chemical exergy with depending of r_{sb} is different during combustion thanks to the different combustion durations as seen in Table 2.

Fig. 9 shows the variation of total exergy with r_{sb}. As seen in the figure, total exergy changes with the variation of r_{sb} during combustion and expansion periods, while it is about the same for all of r_{sb} during compression period. The variations in total exergy are mainly sourced from the variations in thermomechanical exergy and fuel chemical exergy because total exergy is the sum of them. The exergy remained at the end of the expansion period is called as exhaust or waste exergy which is transferred with exhaust gases. As seen in Fig. 9, exhaust exergy decreases with the increase of r_{sb}. The decrements in X_{exh} are about 4 and 4.9 % for r_{sb} of 1.0 and 1.3 in compared with that of r_{sb}=0.7. Fig. 10(a) shows the variation of the first and second law efficiencies and Fig. 10(b) the variation of engine torque and brake specific fuel consumption depending on the r_{sb}, respectively.

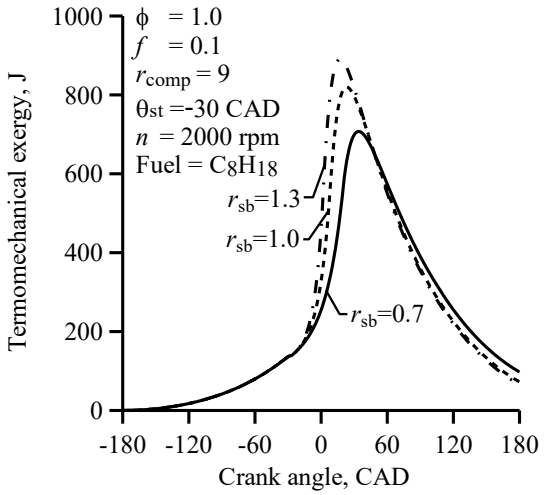

Fig. 7. Effects of r_{sb} on the thermomechanical exergy

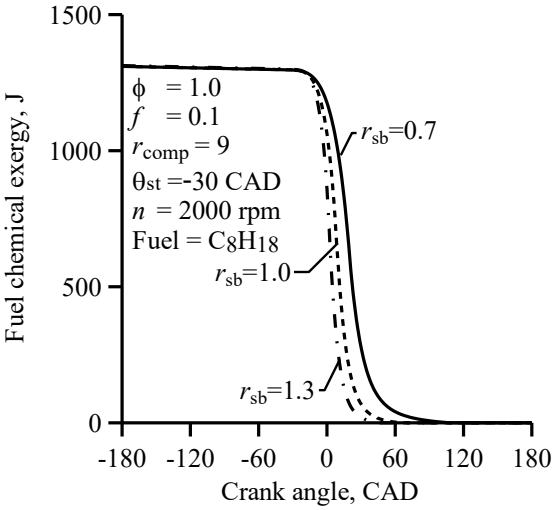

Fig. 8. Effects of r_{sb} on the fuel chemical exergy

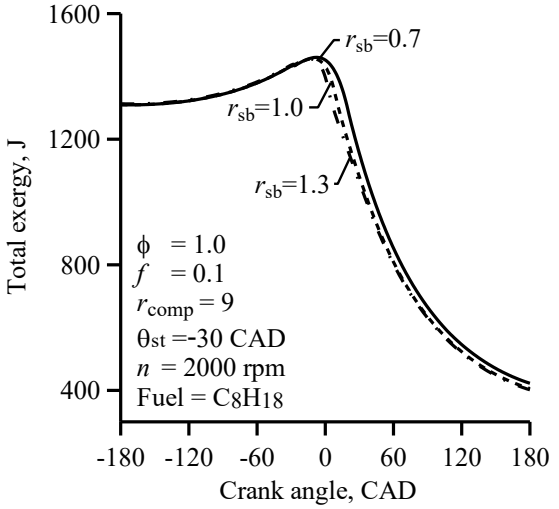

Fig. 9. Effects of r_{sb} on the total exergy

The first and second law efficiency and engine torque increase while brake specific fuel consumption decreases with the increasing of r_{sb} as seen in the figures. It is estimated that the increments in the efficiencies are sourced from the increase of the engine work output i.e. engine torque with the increase of r_{sb}. The increments in the efficiencies are about 9.2 and 12.3 % for r_{sb} of 1.0 and 1.3 in compared with that of r_{sb}=0.7. The increase of the efficiency provides lower brake specific fuel consumption as seen in Fig. 10 (b). The decrements in brake specific fuel consumption are about 8.7 and 11.3 % for r_{sb} of 1.0 and 1.3 in compared with that of r_{sb}=0.7.

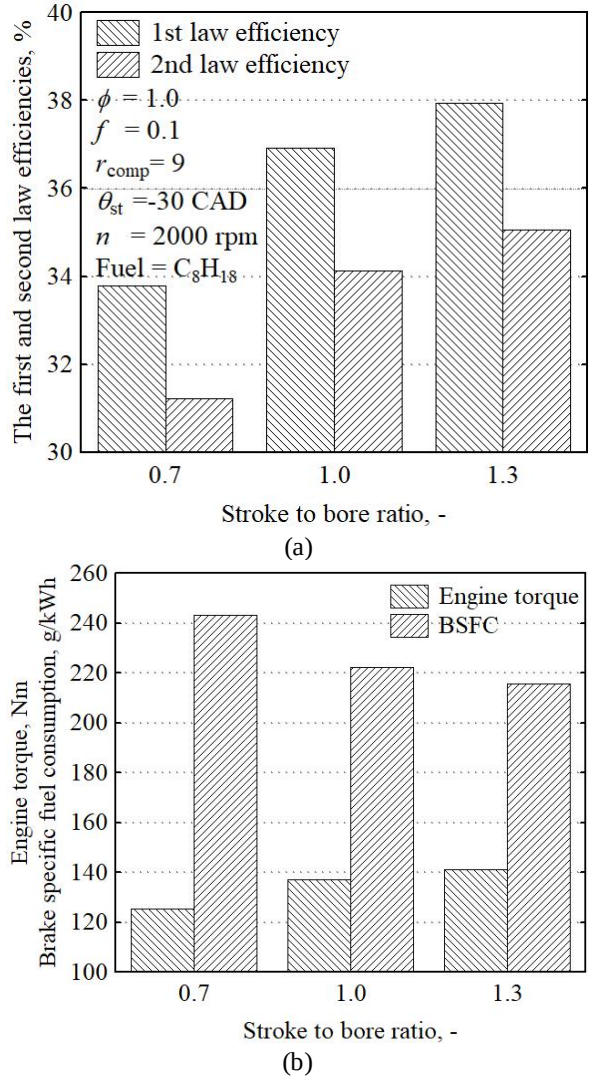

Fig. 10. Effects of r_{sb} on (a) the efficiencies and (b) engine torque and brake specific fuel consumption

6. Conclusions

In order to investigate the compression, combustion and expansion processes of a spark–ignition engine from the second law perspective namely exergy analysis, a thermodynamic–based cycle model was developed. By using this model, the effects of stroke to bore ratio on the variation of exergetic terms and irreversibilities have been investigated theoretically during the mentioned part of the cycle. The effects of stroke to bore ration on the first and second law efficiencies and brake specific fuel consumption are also investigated in the present study. The following general conclusions have been drawn from the results of the study;

- A parametric exergetic analysis provides a better understanding of interactions between some operating conditions, and energy conversion and transfer processes; permits the revelation of the magnitude of work potential lost during the cycle in a more realistic way than the first law analysis can; and points to several possible ways for improving engine performance.
- Exergy transfer with work increases while exergy transfer with heat decreases with increasing of stroke to bore ratio. Maximum increment in exergy transfer with work is about 12.5% and maximum decrement in exergy transfer with heat is about 11.25% for the stroke to bore ratio of 1.3 in comparison with that of stroke to bore ratio of 0.7.
- Both of the irriversibilities and exergy transfer with exhaust decrease with the increasing of stroke to bore ratio. Maximum decrements are about 3.1% in the irriversibilities and 4.9% in exergy transfer with exhaust for the stroke to bore ratio of 1.3 in comparison with that of stroke to bore ratio of 0.7.
- The first and second law efficiencies are increase, while the brake specific fuel consumption decreases with the increase of the stroke to bore ratio. Maximum increments are about 12.3% in the first and second law efficiencies and maximum decrement is about 11.3% in brake specific fuel consumption for the stroke to bore ratio of 1.3 in comparison with that of stroke to bore ratio of 0.7.
- According to obtained results, it can be said that the increase of stroke to bore ratio up to a certain value makes an engine more efficient and economical in terms of fuel consumption.

CRediT authorship contribution statement

Since the article has a single author, all contributions belong to the responsible author.

Declaration of Competing Interest

Since the article has only one author, there is no conflict of interest.

Abbreviations

ATDC : after top dead center
BDC : bottom dead center
BMEP : brake mean effective pressure
BSFC : brake specific fuel consumption
BTDC : before top dead center
BTE : brake thermal efficiency
CAD : crank angle degree
ECU : electronic control unit
ICE : internal combustion engine
SI : spark ignition

Nomenclature

A : area, m^2
A_b : wetted area by burned gas, m^2
A_f : area of flame front, m^2
$A_{iv,max}$: maximum opening area of intake valve, m^2
A_u : wetted area by unburned gas, m^2
C_p : specific heat at constant pressure, J/kgK
d_{iv} : intake valve diameter, m
D_c : diameter (bore) of cylinder, m
e : specific energy, J/kg
E : energy, J
f : mass fraction of residual gas, dimensionless
h : height, m or specific enthalpy, J/kg
I : irreversibilities, J
l_T : characteristic length scale of turbulent flame, m
L_{cr} : connecting rod length, m
$L_{iv,max}$: maximum intake valve lift, m
L_s : stroke length, m
m : mass, kg
n : engine speed, rpm
p : pressure, bar
Q : heat, J
Q_{LVH} : lower heating value of fuel, kJ/kg
Q_{cw} : total heat transfer from the cylinder wall, J
r : radius, m or ratio, dimensionless
r_f : flame radius, m
r_{comp} : compression ratio, dimensionless
r_{mbf} : mass fraction burned ratio, dimensionless
r_{rg} : molar fraction of residual gas, dimensionless
r_{sb} : stroke to bore ratio, dimensionless
r_{sp} : spark plug location ratio, dimensionless
R : cylinder radius, m
R_{sp} : radius of spark plug location from the cylinder axis, m
s : specific entropy, J/kgK
S : entropy, J/K
T : absolute temperature, K
U : speed, m/s
v : specific volume, m^3/kg
V : volume, m^3
V_{cc} : volume of combustion chamber, m^3
V_f : enflamed volume, m^3

x : specific exergy, J/kg
X : exergy, J
X_{exh} : exergy transfer with exhaust gases, J
$X_{f,ch}$: fuel chemical exergy, J
X_Q : exergy transfer with heat, J
X_{tm} : thermomechanical exergy, J
X_W : exergy transfer with work, J
X_{tot} : total exergy, J

Greek letters

ε : error ratio, dimensionless
ϕ : fuel–air equivalence ratio, dimensionless
γ_{sc} : coefficient of supercharge
η_I : first law efficiency, %
η_{II} : second law efficiency, %
η_v : volumetric efficiency, %
λ : heat transfer coefficient
μ : chemical potential, J/kg
θ : crank angle, °
θ_{bd} : burn (combustion) duration, °
θ_{st} : spark timing crank angle, °
ρ : density, kg/m^3
τ_b : characteristic burning time of eddy at size of l_T, s
ω : angular speed, s^{-1}

Subscripts

0 : reference or dead state

conditions
int : internal conditions
b : burned
bd : burn (combustion) duration
c : cylinder
cc : combustion chamber
ch : cylinder head
chem : chemical
cr : connecting rod
comb : combustion
comp : compression
cf : cooling fluid
cw : cylinder wall
dest : destruction
e : entrainment
exh : exhaust
f : flame
g : gas
ind : induction
kin : kinetic
L : laminar
max : maximum
pc : piston crown
pot : potential
rg : residual gas
s : stroke
sb : stroke to bore
sc : supercharge
sp : spark plug
st : spark timing
tm : termomechanical
tot : total
T : turbulent
u : unburned
w : wall

7. References

1. Khoa N. X., Nhu Q. and Lim O., "Estimation of parameters affected in internal exhaust residual gases recirculation and the influence of exhaust residual gas on performance and emission of a spark ignition engine," Applied Energy, 278, 115699, 2020.
2. Ozcan H. and Yamin J. A. A., "Performance and emission characteristics of LPG powered four stroke SI engine under variable stroke length and compression ratio," Energy Conversion and Management, 49, 1193–1201, 2008.
3. Poulos S. G. and Heywood J. B., "The effect of chamber shape on spark ignition engine combustion," Society of Automotive Engineering, SAE paper no 830334, 1–27, 1983.
4. Sung N. W. and Jun S. P., "The effects of combustion chamber geometry in an SI engine", Society of Automotive Engineering, SAE paper no 972996, 227–239, 1997.
5. Filipi Z. S. and Assanis D. N., "The effect of the stroke–to–bore ratio on combustion, heat transfer and efficiency of a homogeneous charge spark ignition engine of given displacement," International Journal of Engine Research, 1(2), 191–208, 2000.
6. Sher E. and Bar–Kohany T., "Optimization of variable valve timing for maximizing performance of an unthrottled SI engine–a theoretical study," Energy, 27, 757–775, 2002.
7. Hu Z., Whitelaw J. H. and Vafidis C., "Flame propagation studies in a four–valve pentroof–chamber spark ignition engine," Society of Automotive Engineering, SAE paper no 922321, 1–11, 1992.
8. Caton J. A., "Detailed results for nitric oxide emissions as determined from a multiple–zone cycle simulation for a spark–ignition engine," Fall Technical Conference of the ASME, Internal Combustion Engine Division, New Orleans, Los Angeles, pp. 1–19, 2002.
9. Rakopoulos C. D. and Giakoumis E. G., "Second law analyses applied to internal combustion engines operation," Progress in Energy and Combustion Science, 32(1), 2–47, 2006.
10. Moran M. J. and Shapiro H. N., "Fundamentals of engineering thermodynamic," New York: John Wiley & Sons Inc., 2000.
11. Caton J. A., "A review of investigations using the second law of thermodynamics to study internal–combustion engines," SAE World Congress, Detroit, Michigan, pp. 1–15, 2000.
12. Rakopoulos C. D., "Evaluation of a spark ignition engine cycle using first and second law analysis techniques," Energy Conversion and Management, 34(12), 1299–1314, 1993.
13. Gallo W. L. R. and Milanez L. F., "Exergetic analysis of ethanol and gasoline fueled engines," Society of Automotive Engineers, SAE paper no 920809, 907–915, 1992.
14. Shapiro H. N. and Van Gerpen J. H.,

"Two zone combustion models for second law analysis of internal combustion engines," Society of Automotive Engineers, SAE paper no 890823, 1408–1422, 1989.
15. Alasfour F. N., "Butanol–a single–cylinder engine study: exergy analysis," Applied Thermal Engineering, 17(6), 537–549, 1997.
16. Caton J. A., "Results from the second–law of thermodynamics for a spark–ignition engine using a cycle simulation," Fall Technical Conference of the ASME, Internal Combustion Engine Division, Ann Arbor, Michigan, pp. 35–49, 1999.
17. Caton J. A., "Operation characteristics of a spark–ignition engine using the second law of thermodynamics: effects of speed and load," SAE World Congress, Detroit, Michigan, pp. 1–17, 2000.
18. Sohret Y., Gürbüz H. and Akçay I. H., "Energy and exergy analyses of a hydrogen fueled SI engine: effect of ignition timing and compression ratio," Energy, 175, 410–422, 2019.
19. Sezer I. and Bilgin A., "Exergy analysis of SI engines," International Journal of Exergy, 5(2), 204–217, 2008.
20. Ferguson C. R., "Internal combustion engine, applied thermosciences," New York: John Wiley & Sons Inc., 1985.
21. Sezer I., "Application of exergy analysis to spark ignition engine cycle," PhD Dissertation, Blacksea Technical University, Trabzon, Turkey, 2008.
22. Blizard N. C. and Keck J. C., "Experimental and theoretical investigation of turbulent burning model for internal combustion engines," Society of Automotive Engineers, SAE Paper no 740191, 846–864, 1974.
23. Keck J. C., "Turbulent flame structure and speed in spark–ignition engines," International Nineteenth Symposium on Combustion, the Combustion Institute, 19(1), 1451–1466, 1982.
24. Tabaczynski R. J., Ferguson C. R. and Radhakrishnan K., "A turbulent entrainment model for spark–ignition combustion," Society of Automotive Engineers, SAE paper no 770647, 2414–2432, 1977.
25. Tabaczynski R. J., Trinker F. H. and Sahnnon B. A. S., "Further refinement of a turbulent flame propagation model for spark–ignition engines," Combustion and Flame, 39, 111–121, 1980.
26. Bayraktar H. and Durgun O., "Mathematical modeling of spark–ignition engine cycles," Energy Sources, 25, 651–666, 2003.
27. Gülder Ö., "Correlations of laminar combustion data for alternative S.I. engine fuels," Society of Automotive Engineers, SAE paper no 841000, 1–23, 1984.
28. Bilgin A., "Geometric features of the flame propagation process for an SI engine having dual–ignition system," International Journal of Energy Research, 26, 987–1000, 2002.
29. Cengel Y. A. and Boles M. A., "Thermodynamics, an engineering approach: 2nd edition," New York: McGraw–Hill Inc., 1994.
30. Rezac P. and Metghalchi H., "A brief note on the historical evolution and present state of exergy analysis," International Journal of Exergy, 1(4), 426–437, 2004.
31. Van Gerpen J. H. and Shapiro H. N., "Second law analysis of diesel engine combustion," Transaction of ASME Journal of Engineering Gas Turbines and Power, 112, 129–137, 1990.
32. Caton J. A., "Results from the second–law of thermodynamics for a spark–ignition engine using a cycle simulation," Proceedings of the ASME–ICED Fall Technical Conference, Ann Arbor, Michigan, pp. 35–49, 1999.
33. Caton J. A., "Operation characteristics of a spark–ignition engine using the second law of thermodynamics: effects of speed and load," SAE World Congress, Detroit, Michigan, pp. 1–17, 2000.
34. Zhang S., "The second law analysis of a spark ignition engine fueled with compressed natural gas," MS Dissertation, University of Windsor, Ontario, Canada, 2002.
Kotas T. J., "The exergy method of thermal plant analysis," Malabar: Krieger Publishing, 1995.